Discovering the Dynamics of the Divisome

Claudia Parker

Supervisors: Professor Phillip Stansfeld and Dr Juliana Vilachã

Introduction

All bacteria must divide, making cell division a promising antibiotic target. At the centre of this lies an important protein complex: the Divisome (Fig. 1), consisting of the proteins FtsW, FtsI, FtsQ, FtsL and FtsB, alongside others[1]. The peptidoglycan cell wall is a core component of the bacterial cell, and FtsW is a glycosyltransferase which synthesises new peptidoglycan, using lipid II as a substrate with C55-PP produced as a product, during bacterial cell division[2]. FtsI is a transpeptidase which cross-links these new peptidoglycan chains, forming a mesh which is connected to the existing cell wall[2]. The exact roles of FtsQLB are unclear but they are thought to stabilise the FtsWI complex[3]. The filament-forming[4] protein FtsA has been suggested to activate FtsW[5].

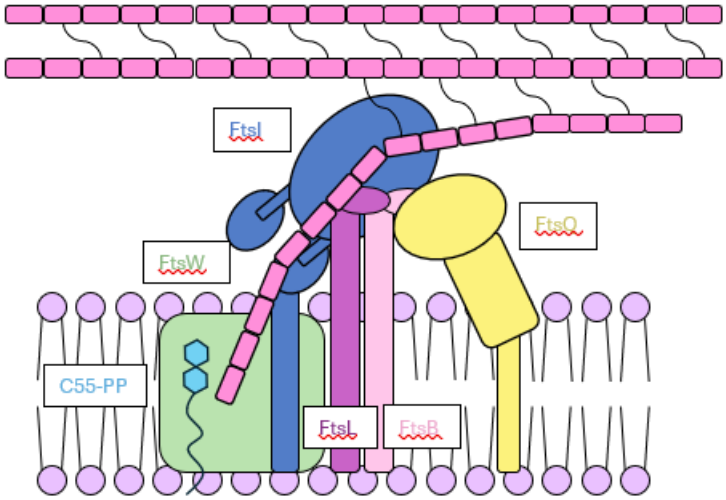

Figure 1. Schematic of peptidoglycan synthesis by FtsW and FtsI in the presence of FtsQLB. New peptidoglycan strands (pink) are synthesised by FtsW (green) with C55-PP released as a product (light blue). The transpeptidase FtsI (dark blue) then cross-links the newly synthesised peptidoglycan strands and they are added to the existing cell wall. FtsQLB (yellow, purple and pink respectively) stabilise FtsI in its active, upright conformation.

Molecular dynamics (MD) simulations are a powerful tool to study protein interactions, complementing experimental data. Previous experimental studies have identified important amino acid residues (Table 1) surrounding a potential active site in both FtsW and its homologue RodA, which is involved in maintaining bacterial cell shape, in *Escherichia coli*[6,7]. Cryo-electron microscopy studies have experimentally determined the structure of the FtsWIQLB complex in *Pseudomonas aeruginosa*[8,9]. These data together show the structure and hint towards a potential mechanism of the FtsWIQLB complex. A simulation of the FtsWIQLB complex in *E. coli* has already been carried out[3], looking at conformational changes within the whole complex, which provide some insight into different protein interactions. To expand on this, I used MD simulations to study the interactions of the FtsWIQLB complex at the structural level, with a focus on FtsW.

E. coli RodA	*E. coli* FtsW	*P. aeruginosa* FtsW
N/A	R73	A49
R48	R84	R60
K97	K133	N111
R101	R137	R115
W102	W138	W116
D104	D140	G118
R109	R145	N123
Q111	Q147	Q125
R210	R246	R224
E254	E289	F267
E258	E293	E271
D262	D297	D275
V331	K370	K348

corresponding residues in *E. coli* FtsW and *P. aeruginosa* FtsW. Residues highlighted to be of importance in previous experimental studies[6,7] or identified in this study.

Aims

To use MD simulations to study the interactions between different Divisome proteins to understand how they function and how we can target them using antibiotics.

Methods

AlphaFold3[10] and SWISS-MODEL[11] homology models of FtsW in *E. coli* and *P. aeruginosa* were generated and their MolProbity[12] and QMEANDisCo[13] scores compared. AlphaFold3 models were used in simulations. Coarse-grained (CG) systems in periodic boxes were set up using MemProtMD[14] and Insane[15] with a lipid bilayer ratio 7:2:1 of POPE:POPG:Cardiolipin. Martinize2[16] was used to create elastic networks. CG systems were converted to atomistic systems for simulation using the CG2AT program's 'align' feature[17]. Production runs of 500 ns for atomistic simulations and 10 µs for CG simulations were carried out using GROMACS 2023.3[18], CHARMM36[19] and a Martini3[20] forcefield and a TIP3P[21] water model. Three repeats of atomistic simulations and one repeat of CG simulations were carried out. PyMOL 2.5.7[22] was used to visualise simulations. Backbone RMSD and RMSF analysis was carried out and VMD 1.9.4a57[23] was used for salt bridge analysis. Lipid II and C55-PP were visualised with FtsW using PyMOL and after simulation MDAnalysis[24,25] used to identify lipid contacts.

MemProtMD[14] and WebLogo3[26] were used for conservation, electrostatic and hydrophobicity analysis. MMseqs2[27] and T-COFFEE[28] were used to generate multiple sequence alignments (MSAs).

Results

Characterisation of Residues Surrounding the Potential FtsW Active Site

Structural analysis of FtsW in *E. coli* and *P. aeruginosa* revealed that, like RodA, FtsW contains two electrostatic cavities with the surrounding residues highly conserved (Fig. 2). Backbone RMSF calculated from atomistic simulations revealed fluctuations in these residues (Fig. 3A-B). Further atomistic simulations of FtsW in *E. coli* and *P. aeruginosa* with lipid II and C55-PP visualised in PyMOL were carried out, and backbone RSMF values revealed that fewer fluctuations occurred when lipid II and C55-PP were bound (Fig. 3C-D). Lipid II and C55-PP also made the most contacts with the residues surrounding the two cavities (Fig. 4). This indicates that these residues could be involved in substrate binding.

Residues surrounding the two cavities were identified and mapped to the structure of FtsW in *E. coli* (Fig. 5). WebLogos were generated to show the conservation of residues, with residues W138, Q147, R246 and D297 being highly conserved (Fig. 5). These have been identified previously as having an important catalytic role in lipid II polymerisation[6]. The residue K133 has been highlighted as important but not for catalysis[6]. Its interactions with both C55-PP and lipid II suggest that it likely plays a role in substrate binding. A T-COFFEE MSA identified the equivalent residues in *E. coli* RodA and *P. aeruginosa* FtsW and these mapped to the same positions in the structures. Salt-bridge analysis revealed a decrease in the interactions of these residues with each other when lipid II and C55-PP were present (Table 2), suggesting that these residues interact with lipid II and C55-PP. As two molecules of lipid II are required for polymerisation[7], this suggests that the cavities form two substrate binding sites in FtsW.

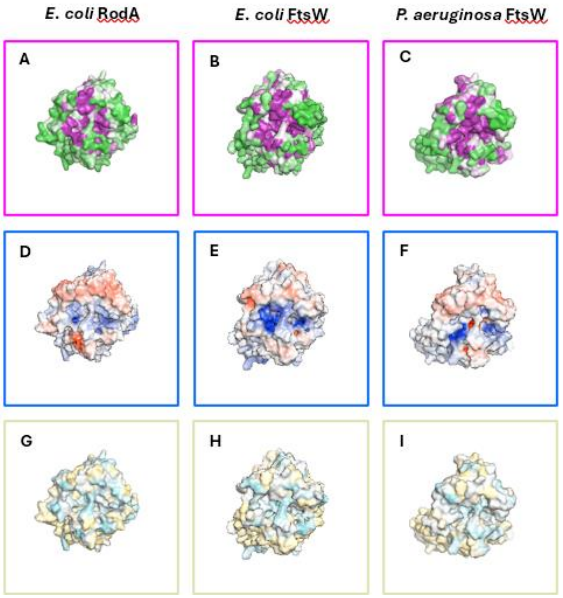

Figure 2. Conservation, electrostatic and hydrophobicity analysis of amino acid residues in RodA and FtsW in *E. coli*, and FtsW in *P. aeruginosa*. A-C. Electrostatic analysis of residues in *E. coli* RodA and FtsW and *P. aeruginosa* FtsW. Dark blue indicates positively charged residues whereas red indicates negatively charged residues. Neutral residues are shown in white. In all proteins, two positively charged cavities can be seen, although this is most pronounced in *E. coli* FtsW and more pronounced in both FtsW proteins compared to RodA. Charged cavities indicate potential binding sites. **D-F.** Conservation analysis of amino acid residues in *E. coli* RodA and FtsW and *P. aeruginosa* FtsW. Purple indicates highly conserved residues, whereas green indicates less conserved residues. Residues present in the charged cavities seen in **A-C** are highly conserved. **G-I.** Hydrophobicity analysis of amino acid residues present in *E. coli* and *P. aeruginosa* FtsW. Cyan indicates hydrophilic residues whilst gold indicates hydrophobic residues. Residues surrounding the cavities seen in **A-C** appear to be hydrophilic.

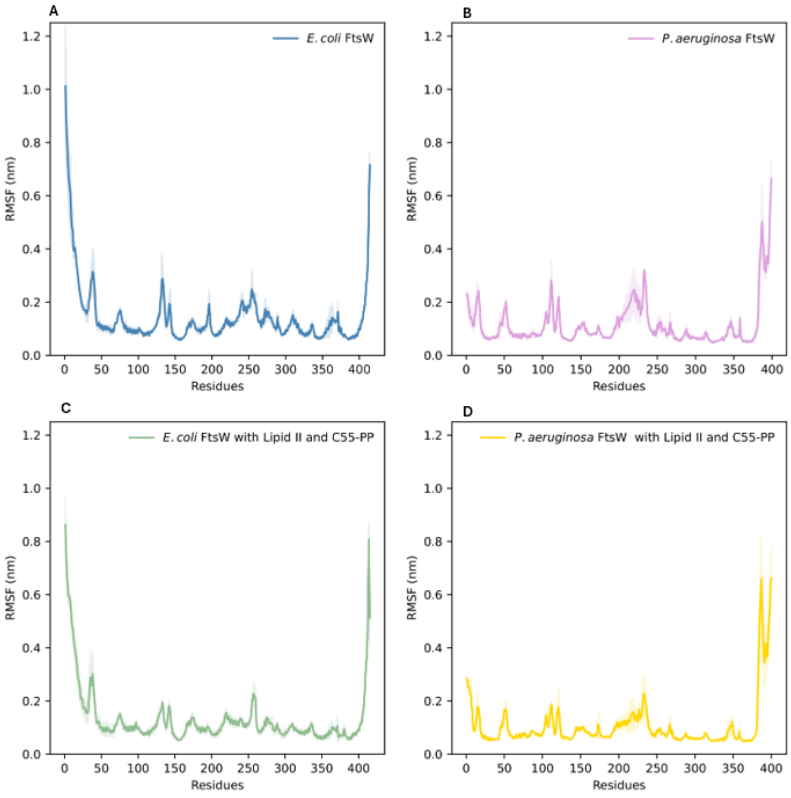

Figure 3. Mean and standard deviation of RMSF values of FtsW in *E. coli* and *P. aeruginosa* from three repeats each of 500 ns atomistic simulations with and without Lipid II and C55-PP bound. A. Mean and standard deviation of backbone RMSF in *E. coli* FtsW. **B.** Mean and standard deviation of backbone RMSF in *P. aeruginosa* FtsW. **C.** Mean and standard deviation of backbone RMSF in *E. coli* FtsW with Lipid II and C55-PP bound. **D.** Mean and standard deviation of backbone RMSF in *P. aeruginosa* FtsW with Lipid II and C55-PP bound. Residues are shown on the X-axis and RMSF on the Y-axis. Standard deviation is shown as shading. Peaks indicate increased fluctuations of the corresponding residues on the X-axis.

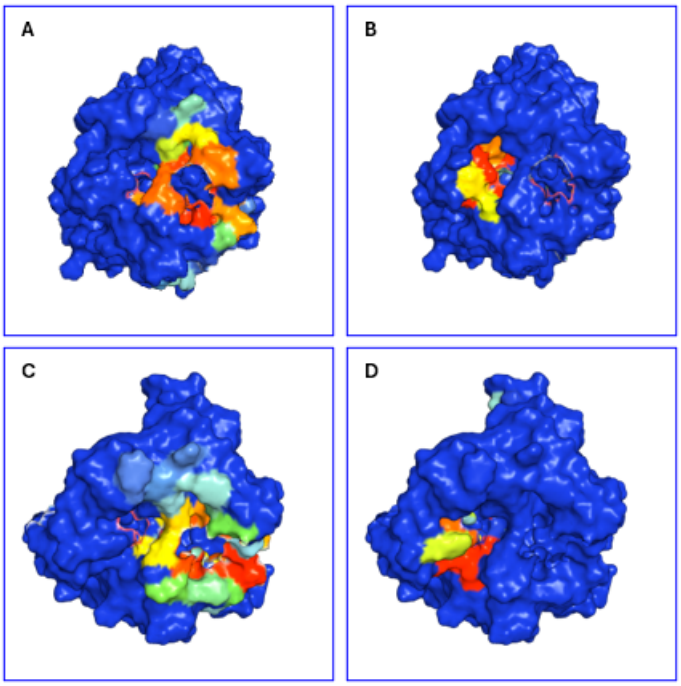

Figure 4. Lipid II and C55-PP contacts with FtsW in *E. coli* and *P. aeruginosa* 500 ns atomistic simulations. A. Lipid II contacts with FtsW in *E. coli*. Residues are coloured by B-factor with residues coloured red having the most contact with lipid II and residues shown in dark blue having no contact with lipid II. **B.** C55-PP contacts with FtsW in *E. coli*. Residues coloured red have the most contact with C55-PP and residues coloured dark blue make no contacts with C55-PP. **C.** Lipid II contacts with FtsW in *P. aeruginosa*. Residues coloured red make the most contacts with lipid II while residues coloured dark blue make no contacts with lipid II. **D.** C55-PP contacts with FtsW in *P. aeruginosa*. Residues coloured red make the most contacts with C55-PP while residues coloured dark blue make no contacts with C55-PP.

Residues forming bridge	*E. coli*		Residues forming bridge	*P. aeruginosa*	
	Mean % occupancy			Mean % occupancy	
	FtsW alone	FtsW with Lipid II and C55-PP		FtsW alone	FtsW with Lipid II and C55-PP
R73-E289	4.03	45.4	N/A	N/A	N/A
D140-R145	66.8	31.5	N/A	N/A	N/A
K133-E293	45.4	29.7	N/A	N/A	N/A
E293-K370	86.3	21.0	E271-K348	94.0	47.7
D297-K370	88.2	15.4	D275-K348	84.1	44.1

Table 2. Mean percentage occupancy of salt bridges formed between different residues in FtsW in *E. coli* and *P. aeruginosa* with and without lipid II and C55-PP present. Data was calculated using three repeats of 500 ns atomistic simulations of FtsW in *E. coli* and *P. aeruginosa* with and without lipid II and C55-PP present.

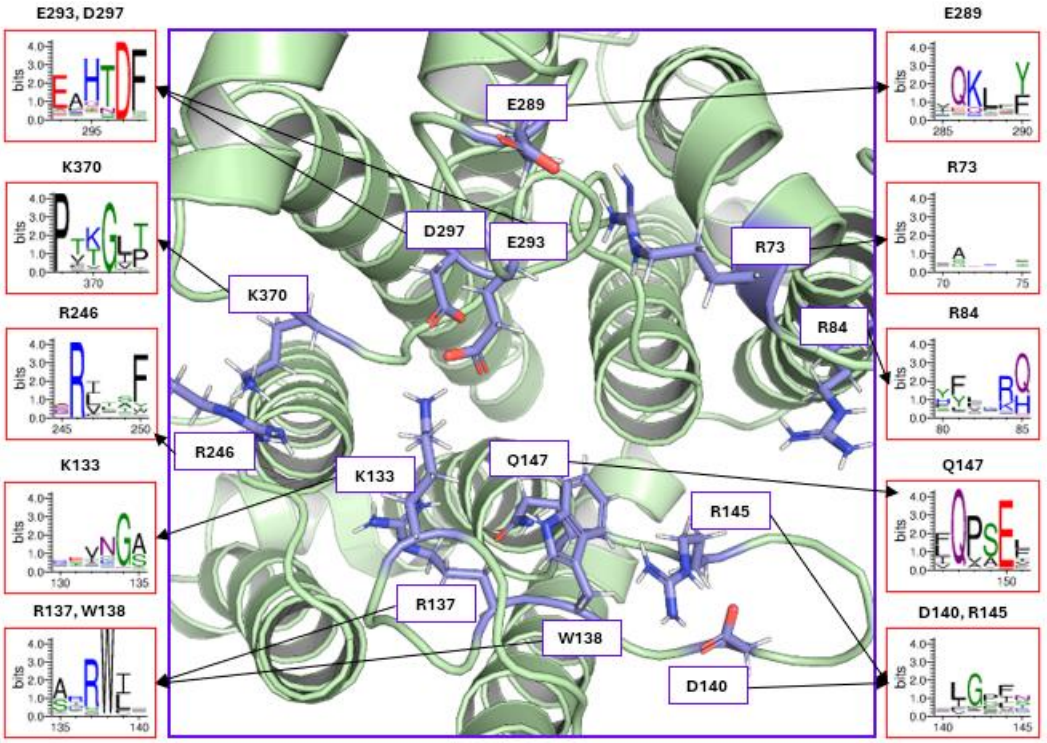

Figure 5. Conservation of important residues surrounding the cavities of FtsW in *E. coli*. Thirteen residues were identified as having a potential role in the mechanism of FtsW either from salt-bridge analysis or previously published experimental data[6,7] about RodA and FtsW in *E. coli* (residues are coloured purple and named using white text boxes with black borders). Weblogos (graphs outside the central figure showing one-letter amino acid codes) were generated to visualise residue conservation. Black arrows point from residues to their corresponding Weblogo plot. X-axis of the Weblogo plots shows the protein's primary sequence, with the residues on the graph. Y-axis shows conservation. Taller letters indicate a higher degree of conservation. Residues W138, Q147, R246 and D297 are highly conserved.

Interactions of FtsWA

Atomistic simulations of FtsWA revealed that FtsW adopts a more open conformation when FtsA is present (Fig. 6) and that FtsA forms a β-sheet with FtsW (Fig. 7). It has been shown that FtsA forms an anti-parallel filament[4] and hypothesised that it activates FtsW with the involvement of FtsN[5]. A further 10 μs CG simulation of the FtsWIQLB complex with four copies of FtsA, and FtsN residues 1-32 and 75-93, also revealed that FtsW adopted a more open conformation compared to CG simulations of the FtsWIQLB complex alone (Fig. 8). Simulations of FtsW alone revealed it to be a compact protein, and so for lipid II to enter its binding site an open conformation of FtsW is likely needed. The presence of the β-sheet between FtsA and FtsW could play a role in this. Overall, this suggests that FtsA potentially activates FtsW which then adopts an open conformation.

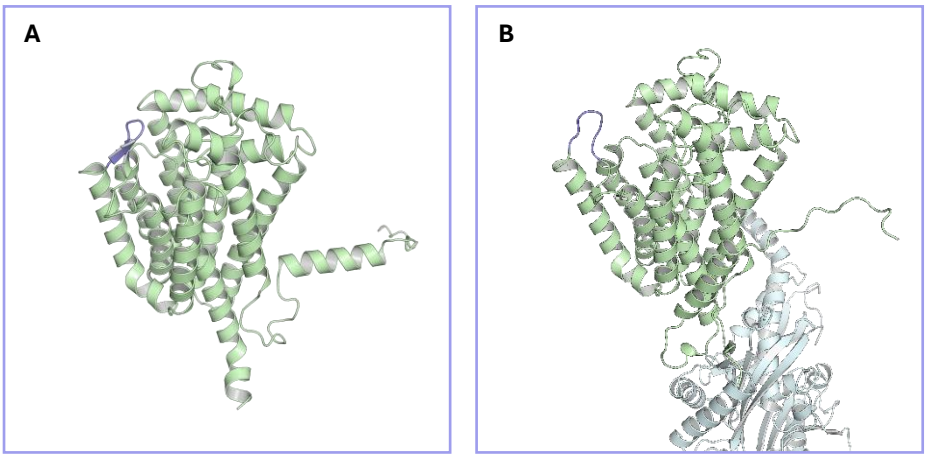

Figure 6. FtsW adopts an open conformation in the presence of FtsA. A. FtsW in a 500 ns atomistic simulation without FtsA present. FtsW adopts a closed conformation with residues 130-136 forming a β-strand and a loop (purple). **B.** FtsW (green) adopts an open conformation in a 500 ns atomistic simulation in the presence of FtsA (cyan). Residues 130-136 (purple) form a loop which opens outwards.

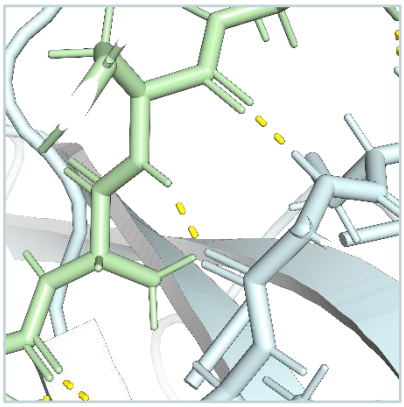

Figure 7. FtsW forms a β-sheet with FtsA. FtsW (green) and FtsA (cyan) in a 500 ns atomistic simulation. Residues 406-414 in FtsW and residues 73-78 in FtsA form a β-sheet with each other.

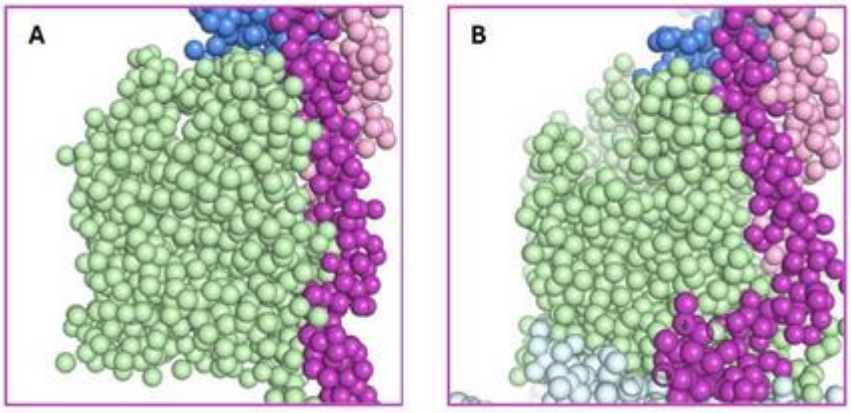

Figure 8. FtsW in the FtsWIQLB complex adopts an open conformation in the presence of FtsA and FtsN. A. FtsW (green) adopts a closed conformation in a 10 μs coarse-grained simulation of the FtsWIQLB complex. **B.** FtsW (green) adopts an open conformation in a 10 μs CG simulation of the FtsWIQLB complex with four copies of FtsA (cyan) and FtsN residues 1-32 and 75-93 (not shown). FtsL is shown in purple, FtsB in pink and FtsI in dark blue.

Interactions of the FtsWIQLB Complex

Atomistic and CG simulations revealed multiple conformational changes in *E. coli* FtsWI (Fig. 9A-B, Fig. 10A-C). In a 10 μs CG simulation of FtsWI, FtsI was seen in an upright position, then falling to the membrane, and then attempting to lift back up (Fig. 10A-C). It was also seen to split into two. Atomistic simulations of *E. coli* FtsWI showed FtsI falling to the membrane and staying there (Fig. 9A-B). This indicates that FtsI requires further proteins to stabilise it in its upright, active position. A 10 μs CG simulation of FtsQLB revealed that FtsQLB also fell to the membrane (Fig. 10D). FtsQLB is thought to stabilise FtsI in the upright position, so this data suggests that both FtsWI and FtsQLB stabilise each other. A further 10 μs CG simulation of FtsWIQLB showed the complex in a more upright position, however FtsI did not extend fully upright, and the complex still fell to the membrane repeatedly (Fig. 10E-F). This data suggests that FtsWIQLB alone are not enough to stabilise FtsI in its active, upright position.

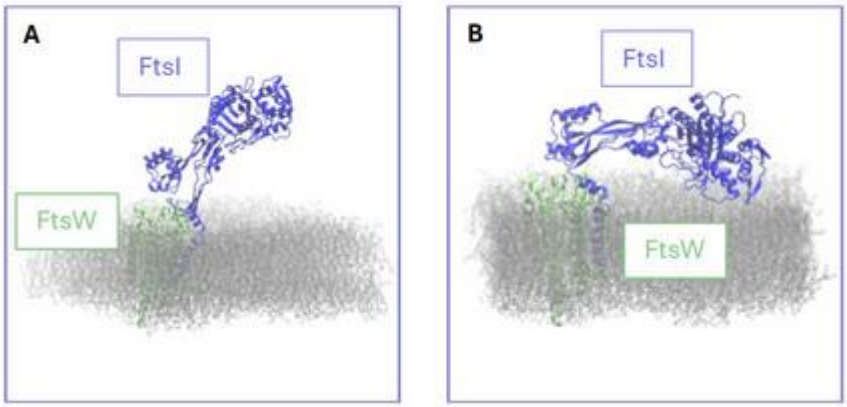

Figure 9. FtsI falls to the membrane in the absence of FtsQLB. A. FtsI (dark blue) begins a 500 ns atomistic simulation in the presence of FtsW (green) in an upright position. **B.** FtsI falls to the membrane (grey) during a 500 ns atomistic simulation.

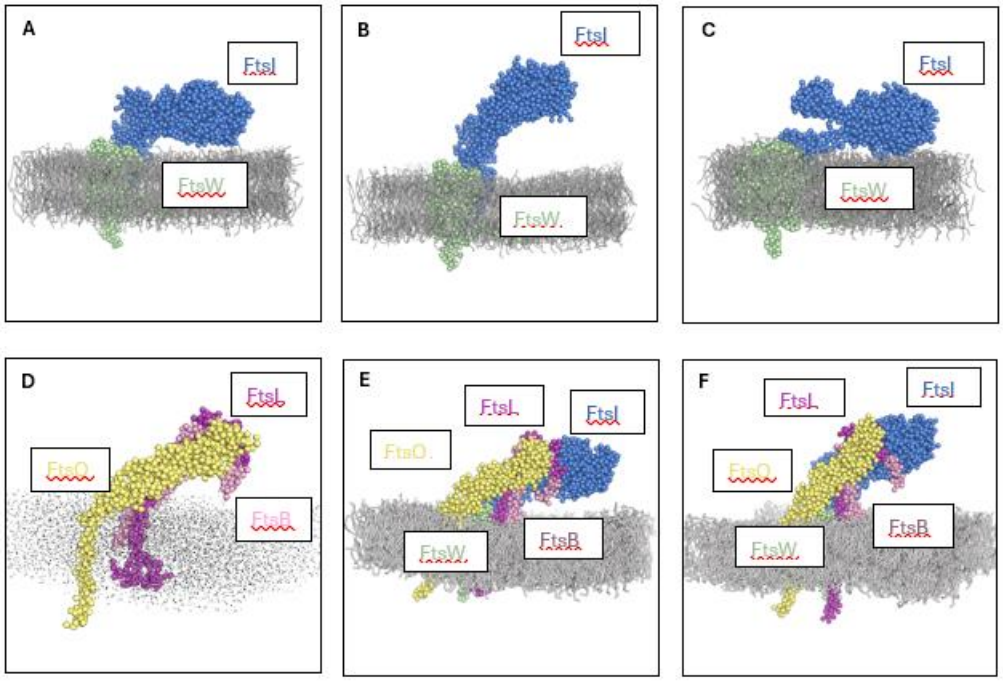

Figure 10. Changes to the FtsWIQLB complex during 10 µs CG simulations. A-C. Conformational changes in FtsI during a 10 µs simulation of the FtsWI complex. FtsI was seen falling to the membrane (**A**), lifting up from the membrane (**B**) and falling to the membrane and opening out (**C**). **D.** FtsQLB falls to the membrane during a 10 µs CG simulation. **E-F.** FtsWIQLB falls to the membrane (**E**) but also adopts a more upright position (**F**) in a 10 µs CG simulation.

Discussion

The Divisome has been characterised as the proteins FtsWIQLB[8,9] however data here shows that they are unlikely to form the whole complex. The interactions between FtsA and FtsW need to be further explored to determine exactly if and how FtsA activates FtsW. If this is known, then it is an antibiotic target.

Previous experimental studies have highlighted the residues W138, Q147, R246 and D297 surrounding the FtsW potential active site as having important catalytic roles in lipid II polymerisation[6]. Other residues such as K133 have been highlighted as important but not for catalysis[6]. Therefore, these residues could have a role in co-ordinating the binding of lipid II in the FtsW active site. A next step would be to simulate FtsW with two copies of lipid II to see how they interact. This project provides a solid foundation for further understanding of how these residues interact with lipid II to identify the exact mechanism of lipid II polymerisation.

Acknowledgements:

I would like to thank Phillip Stansfeld, Juliana Vilachã and the Stansfeld Group for supervising and supporting me throughout this project. I have gained a wide variety of computational skills, including the ability to run both coarse-grained and atomistic molecular dynamics simulations as well as plenty of coding experience. Before this project, I had never coded before, and now I am confident to use my coding skills to run simulations and analyse data. This alongside learning about the scientific research process and having the opportunity to present my research to the group has been invaluable.

In the Stansfeld Group, this project will be taken forward by myself for my Integrated Master's project and by other students. As this was a new project, I gained valuable experience in project design as I had to determine the direction of the project and decide which experiments to prioritise. I was able to work independently and decide what was interesting to investigate further. This has given me the confidence that I can pursue a PhD and drive my own research in the future.

References

1. Cameron, T. A. & Margolin, W. Insights into the assembly and regulation of the bacterial divisome. *Nat Rev Microbiol* **22**, 33–45 (2024).
2. Taguchi, A. *et al.* FtsW is a peptidoglycan polymerase that is functional only in complex with its cognate penicillin-binding protein. *Nat Microbiol* **4**, 587–594 (2019).
3. Britton, B. M. *et al.* Conformational changes in the essential E. coli septal cell wall synthesis complex suggest an activation mechanism. *Nat Commun* **14**, 4585 (2023).
4. Nierhaus, T. *et al.* Bacterial divisome protein FtsA forms curved antiparallel double filaments when binding to FtsN. *Nat Microbiol* **7**, 1686–1701 (2022).
5. Park, K.-T., Pichoff, S., Du, S. & Lutkenhaus, J. FtsA acts through FtsW to promote cell wall synthesis during cell division in Escherichia coli. *Proceedings of the National Academy of Sciences* **118**, e2107210118 (2021).
6. Li, Y. *et al.* Identification of the potential active site of the septal peptidoglycan polymerase FtsW. *PLOS Genetics* **18**, e1009993 (2022).
7. Nygaard, R. *et al.* Structural basis of peptidoglycan synthesis by E. coli RodA-PBP2 complex. *Nat Commun* **14**, 5151 (2023).
8. Käshammer, L. *et al.* Cryo-EM structure of the bacterial divisome core complex and antibiotic target FtsWIQBL. *Nat Microbiol* **8**, 1149–1159 (2023).
9. Yang, L. *et al.* Structural insights into the activation of the divisome complex FtsWIQLB. *Cell Discov* **10**, 1–4 (2024).
10. Abramson, J. *et al.* Accurate structure prediction of biomolecular interactions with AlphaFold 3. *Nature* **630**, 493–500 (2024).
11. Waterhouse, A. *et al.* SWISS-MODEL: homology modelling of protein structures and complexes. *Nucleic Acids Research* **46**, W296–W303 (2018).
12. Chen, V. B. *et al.* MolProbity: all-atom structure validation for macromolecular crystallography. *Acta Crystallogr D Biol Crystallogr* **66**, 12–21 (2010).
13. Studer, G. *et al.* QMEANDisCo—distance constraints applied on model quality estimation. *Bioinformatics* **36**, 1765–1771 (2020).
14. Newport, T. D., Sansom, M. S. P. & Stansfeld, P. J. The MemProtMD database: a resource for membrane-embedded protein structures and their lipid interactions. *Nucleic Acids Research* **47**, D390–D397 (2019).
15. Wassenaar, T. A., Ingólfsson, H. I., Böckmann, R. A., Tieleman, D. P. & Marrink, S. J. Computational Lipidomics with insane: A Versatile Tool for Generating Custom Membranes for Molecular Simulations. *J. Chem. Theory Comput.* **11**, 2144–2155 (2015).
16. de Jong, D. H. *et al.* Improved Parameters for the Martini Coarse-Grained Protein Force Field. *J. Chem. Theory Comput.* **9**, 687–697 (2013).
17. Vickery, O. N. & Stansfeld, P. J. CG2AT2: an Enhanced Fragment-Based Approach for Serial Multi-scale Molecular Dynamics Simulations. *J. Chem. Theory Comput.* **17**, 6472–6482 (2021).
18. Abraham, M. J. *et al.* GROMACS: High performance molecular simulations through multi-level parallelism from laptops to supercomputers. *SoftwareX* **1**, 19–25 (2015).
19. Huang, J. & MacKerell Jr, A. D. CHARMM36 all-atom additive protein force field: Validation based on comparison to NMR data. *Journal of Computational Chemistry* **34**, 2135–2145 (2013).
20. Souza, P. C. T. *et al.* Martini 3: a general purpose force field for coarse-grained molecular dynamics. *Nat Methods* **18**, 382–388 (2021).
21. Jorgensen, W. L., Chandrasekhar, J., Madura, J. D., Impey, R. W. & Klein, M. L. Comparison of simple potential functions for simulating liquid water. *The Journal of Chemical Physics* **79**, 926–935 (1983).
22. Schrödinger, LLC. The PyMOL Molecular Graphics System, Version 2.5.7. (2015).
23. Humphrey, W., Dalke, A. & Schulten, K. VMD – Visual Molecular Dynamics. *Journal of Molecular Graphics* **14**, 33–38 (1996).
24. Michaud-Agrawal, N., Denning, E. J., Woolf, T. B. & Beckstein, O. MDAnalysis: A Toolkit for the Analysis of Molecular Dynamics Simulations. *J Comput Chem* **32**, 2319–2327 (2011).
25. Gowers, R. J. *et al.* MDAnalysis: A Python Package for the Rapid Analysis of Molecular Dynamics Simulations. in *Proceedings of the 15th Python in Science Conference* (eds. Benthall, S. & Rostrup, S.) 98–105 (2016). doi:10.25080/Majora-629e541a-00e.
26. Crooks, G. E., Hon, G., Chandonia, J.-M. & Brenner, S. E. WebLogo: A Sequence Logo Generator. *Genome Res.* **14**, 1188–1190 (2004).
27. Steinegger, M. & Söding, J. MMseqs2 enables sensitive protein sequence searching for the analysis of massive data sets. *Nat Biotechnol* **35**, 1026–1028 (2017).
28. Notredame, C., Higgins, D. G. & Heringa, J. T-coffee: a novel method for fast and accurate multiple sequence alignment1. *Journal of Molecular Biology* **302**, 205–217 (2000).